NASA TECHNICAL MEMORANDUM

NASA TM X-52946

NASA TM X-52946

OPTIMIZATION OF CONICAL HYDROSTATIC BEARING FOR MINIMUM FRICTION

by Lester J. Nypan, Bernard J. Hamrock, Herbert W. Scibbe, and William J. Anderson
Lewis Research Center
Cleveland, Ohio

TECHNICAL PAPER proposed for presentation at Joint Lubrication Conference sponsored by the American Society of Mechanical Engineers and the American Society of Lubrication Engineers
Pittsburgh, Pennsylvania, October 5-7, 1971

OPTIMIZATION OF CONICAL HYDROSTATIC BEARING FOR MINIMUM FRICTION

by Lester J. Nypan,* Bernard J. Hamrock, Herbert W. Scibbe, and William J. Anderson

Lewis Research Center

SUMMARY

Equations for the flow rate, load capacity, and friction torque for a conical hydrostatic bearing were developed. These equations were solved by a digital computer program to determine bearing configurations for minimum friction torque. Design curves are presented that show optimal bearing dimensions or minimum friction torque as a function of dimensionless flow rate for a range of dimensionless load capacity. Results are shown for both laminar and turbulent flow conditions.

The results indicate that hydrostatic pocket friction is a significant portion of the total friction torque. However, the bearing dimensions for a minimum friction design are affected very little by inclusion of pocket friction in the analysis. For laminar flow the values of the outer-land radius ratio X_3 and outer bearing radius ratio X_4 did not change significantly with increasing friction factor. For turbulent flow, the outer bearing radius ratio X_4 did not change with increasing friction factor; therefore, the value determined for X_4 in the laminar flow case is valid for all turbulent flows.

INTRODUCTION

The design of incompressible fluid hydrostatic bearings with a variety of bearing configurations has been treated by Rippel (ref. 1) and others (refs. 2 and 3). These analyses have resulted in equations for load capacity, flow rate, and friction torque. References 1 and 2 also indicate optimum bearing proportions to minimize pressurization or pumping power requirements of such bearings. Preliminary studies on combination rolling-element - fluid-film bearings for high-speed applications such as the hybrid

---

* Professor of Engineering, San Fernando Valley State College, Northridge, California; NASA Summer Faculty Fellow in 1970.

boost bearing (ref. 4) or the series hybrid fluid-film - rolling-element bearing (ref. 5) have led to an interest in the design and performance characteristics of a conical hydrostatic bearing optimized to minimize bearing friction torque.

The series hybrid bearing requires a minimum-friction fluid-film bearing in order to obtain the maximum reduction in rotative speed for the rolling-element bearing. The conical hydrostatic bearing was selected for analysis as it has both thrust and radial load capacity without the complexity of separate thrust and journal bearings. Overall film thickness and friction torque of the bearing may be readily modified by changing the supply pressure or, equivalently, the flow rate. This feature makes the conical hydrostatic bearing a prime candidate for use in future experimental work on the series hybrid bearing concept.

This study presents an analysis of a conical hydrostatic bearing optimized to minimize friction and a method of designing such a bearing for various combinations of operating conditions of load capacity, flow rate, and Reynolds number.

Two operating regimes may be identified as of interest in conical hydrostatic bearing design. These are (1) the low- and moderate-speed regime, where laminar flow may be expected under the lands and within the hydrostatic pockets, and (2) the high-speed regime, where turbulent flow might be expected within the hydrostatic pockets.

The method used to predict bearing performance characteristics in each of these cases will be that of expressing equations relating pressure, thrust load, flow, and friction torque in terms of bearing design parameters. Friction torque can then be minimized by equating the rate of change of friction torque with bearing size to zero.

ANALYSIS

Figure 1 shows the configuration of a conical hydrostatic bearing as applied to a series hybrid fluid-film - rolling-element bearing. Figure 2 shows the type of conical hydrostatic bearing considered for this design application. Fluid is introduced at the shaft centerline (fig. 2(a)) and is fed radially to orifice or capillary flow restrictors, at radius R_o, which provide pressure compensation for potential misalinement and varying loads. The hydrostatic pressure available for load capacity is that developed at radius R_o because of centrifugal effects. After the fluid has passed through the compensating element, a pressure p is presumed to be available in the hydrostatic pockets to resist a thrust load F. (Symbols are defined in the appendix.) The required pressure area is determined by the thrust load the bearing must carry at supply pressure p. The load capacity can be expressed by

$$F = \frac{p\pi}{2}\left(R_4^2 + R_3^2 - R_2^2 - R_1^2\right) \tag{1}$$

Equation (1) presumes that the full pressure p acts over the area of the pockets and that the average pressure over the circumferential lands is p/2. This is a good approximation provided that R_4/R_3 and R_2/R_1 are not too much greater than 1. The effects of relative motion on pressure profiles are neglected in this analysis.

Flow will take place radially over each circumferential land. The total flow is the sum of the flow over the lands or

$$Q = Q_i + Q_o = \frac{\pi h_L^3 p \sin\theta}{6\mu}\left(\frac{1}{\ln\frac{R_2}{R_1}} + \frac{1}{\ln\frac{R_4}{R_3}}\right) \tag{2}$$

Friction torque due to the circumferential lands is presumed to be the result of laminar shearing of the fluid between inner and outer circumferential lands and the mating surface. The friction torque due to the inner and outer circumferential lands can be written as

$$M_L = \frac{\pi\mu\omega_f}{2h_L \sin\theta}\left(R_4^4 - R_3^4 + R_2^4 - R_1^4\right) \tag{3}$$

Let

$$X_2 = \frac{R_2}{R_1} \qquad \overline{F} = \frac{2F}{\pi p R_1^2}$$

$$X_3 = \frac{R_3}{R_1} \qquad \overline{Q} = \frac{6\mu Q}{\pi p h_L^3 \sin\theta}$$

$$X_4 = \frac{R_4}{R_1} \qquad \overline{M}_L = \frac{2M_L h_L \sin\theta}{\pi\mu\omega_f R_1^4}$$

equations (1) to (3) can be written in dimensionless form as

$$\overline{F} = X_4^2 + X_3^2 - X_2^2 - 1 \tag{4}$$

$$\overline{Q} = \overline{Q}_i + \overline{Q}_o = \frac{1}{\ln X_2} + \frac{1}{\ln \frac{X_4}{X_3}} \tag{5}$$

$$\overline{M}_L = X_4^4 - X_3^4 + X_2^4 - 1 \tag{6}$$

Solving for X_4 in equation (5) gives

$$X_4 = X_3 \exp\left(\frac{1}{\overline{Q} - \frac{1}{\ln X_2}}\right) \tag{7}$$

Note that X_4 is undefined for $\overline{Q} = 1/\ln X_2$. Substituting equation (7) for X_4 into equations (4) and (6) gives

$$\overline{F} = X_3^2\left[1 + \exp\left(\frac{2}{\overline{Q} - \frac{1}{\ln X_2}}\right)\right] - X_2^2 - 1 \tag{8}$$

$$\overline{M}_L = X_3^4\left[-1 + \exp\left(\frac{4}{\overline{Q} - \frac{1}{\ln X_2}}\right)\right] + X_2^4 - 1 \tag{9}$$

Solving for X_3 in equation (8) gives

$$X_3 = \left[\frac{\overline{F} + X_2^2 + 1}{1 + \exp\left(\frac{2}{\overline{Q} - \frac{1}{\ln X_2}}\right)}\right]^{1/2} \tag{10}$$

$$\overline{M}_L = X_2^4 + \left(\overline{F} + X_2^2 + 1\right)^2 \tanh\left(\frac{1}{\overline{Q} - \frac{1}{\ln X_2}}\right) - 1 \tag{11}$$

$$\frac{d\overline{M}_L}{dX_2} = 4X_2^3 + \left(\overline{F} + X_2^2 + 1\right)\left[4X_2 \tanh\left(\frac{1}{\overline{Q} - \frac{1}{\ln X_2}}\right) - \frac{\left(\overline{F} + X_2^2 + 1\right)}{X_2\left(\overline{Q} \ln X_2 - 1\right)^2} \operatorname{sech}^2\left(\frac{1}{\overline{Q} - \frac{1}{\ln X_2}}\right)\right] \tag{12}$$

Physical Restrictions

From figure 2 and the relations for the dimensionless radii, the following can be written:

$$1 < X_2 < X_3 < X_4 \tag{13}$$

From equation (10) and inequality (13),

$$X_2 < \left[\frac{\overline{F} + X_2^2 + 1}{1 + \exp\left(\frac{2}{\overline{Q} - \frac{1}{\ln X_2}}\right)}\right]^{1/2} \tag{14}$$

A further restriction which one needs in order to get reasonable results is that

$$\overline{Q}_o \geq \overline{Q}_i - \frac{1}{\ln \frac{X_4}{X_3}} > \frac{1}{\ln X_2} - \frac{X_4}{X_3} < X_2 \tag{15}$$

Making use of equation (10), inequality (15) yields

$$X_2 > \exp\left(\frac{2}{\overline{Q}}\right) \tag{16}$$

Making use of equations (14) and (16) while letting $X_2 \rightarrow \exp\left(\frac{2}{\overline{Q}}\right)$ yields

$$e^{2/\overline{Q}} < \left(\frac{\overline{F} + e^{4/\overline{Q}} + 1}{1 + e^{4/\overline{Q}}}\right)^{1/2}$$

The preceding results in the following relation between $\overline{F}$ and $\overline{Q}$:

$$\overline{F} > \exp\left(\frac{8}{\overline{Q}}\right) - 1 \tag{17}$$

Low-Speed Operating Regime

At low speeds pocket friction will occur through laminar shearing of the fluid. The pressure gradient created by the action of the radial lands and pockets will also contribute to friction torque, as has been shown by Shinkle and Hornung (ref. 6). Their experimental results, supports their analytical finding that the effective friction shear stress may be calculated from $f = 2\tau/\rho V^2$ with $f = 8/Re$ in the laminar flow regime ($Re<1000$). For the conical hydrostatic bearing, $Re = \rho r \omega_f h_P/\mu$ and

$$\tau = \frac{4\mu}{h_P} r\omega_f \tag{18}$$

Then

$$M_P = \int_{R_2}^{R_3} r\tau dA = \int_{R_2}^{R_3} r\left(\frac{4\mu r\omega_f}{h_P}\right) f_r\left(\frac{2\pi r\, dr}{\sin\theta}\right)$$

or

$$M_P = \frac{2\pi\mu\omega_f f_r}{h_P \sin\theta}\left(R_3^4 - R_2^4\right) \tag{19}$$

The total fluid-film friction torque is the sum of the friction torque due to the circumferential lands and the pocket friction. This can be expressed as

$$M_t = M_L + M_P \tag{20}$$

By use of equation (19), equation (20) can be written in dimensionless form as

$$\overline{M}_t = \frac{2M_t h_L \sin\theta}{\pi\mu\omega_f R_1^4} = \overline{M}_L + C_1\left(X_3^4 - X_2^4\right) \tag{21}$$

where

$$C_1 = 4f_r \frac{h_L}{h_P} \tag{22}$$

In bearings where friction is to be minimized, the fraction of potential pocket area actually used as hydrostatic pockets f_r will be close to unity. It may then be noted that, for $h_P >> h_L$, $C_1 \cong 0$ and in equation (21) the total friction torque becomes equal to that due to the circumferential lands ($\overline{M}_t = \overline{M}_L$).

Differentiating equation (21) with respect to X_2 results in

$$\frac{d\overline{M}_t}{dX_2} = \frac{d\overline{M}_L}{dX_2} + 4C_1\left(X_3^3 \frac{dX_3}{dX_2} - X_2^3\right) \tag{23}$$

The expression for dX_3/dX_2 can be obtained from equation (10) as

$$\frac{dX_3}{dX_2} = \frac{1}{X_3}\left\{\frac{X_2}{1 + \exp\left(\dfrac{2}{\overline{Q} - \dfrac{1}{\ln X_2}}\right)} + \frac{\left(\overline{F} + X_2^2 + 1\right)\exp\left(\dfrac{2}{\overline{Q} - \dfrac{1}{\ln X_2}}\right)}{X_2\left(\overline{Q}\ln X_2 - 1\right)^2\left[1 + \exp\left(\dfrac{2}{\overline{Q} - \dfrac{1}{\ln X_2}}\right)\right]^2}\right\} \tag{24}$$

Therefore, with equations (10), (12), and (24), equations (21) and (23) are expressed in terms of C_1, X_2, $\overline{F}$, and $\overline{Q}$.

High-Speed Regime

When speeds become large enough to result in Reynolds numbers ($Re = \rho\omega_f R_1 h_L/\mu$) greater than 1000, the turbulent friction action of the hydrostatic pockets must be included.

Bearings operating within the turbulent flow regime have been treated by a number of investigators (refs. 7 to 9). The work of Hirs (ref. 9), however, most accurately represents the experimental work of Shinkle and Hornung (ref. 6) on turbulent hydrostatic bearing friction measurements. The work of these authors was used to derive the shear stress as

$$\tau = 0.031\,\rho V^2\,Re^{-0.25} \tag{25}$$

From equation (25), the friction torque due to the hydrostatic pockets M_P can be calculated by

$$M_P = \int_{R_2}^{R_3} r(0.031)\rho V^2 \left(\frac{\rho r\,\omega_f h_P}{\mu}\right)^{-0.25} f_r\left(\frac{2\pi r\,dr}{\sin\theta}\right) \tag{26}$$

or

$$M_P = \frac{(0.031)2\pi f_r}{4.75\sin\theta}\,\rho^{0.75}\omega_f^{1.75}\left(\frac{\mu}{h_P}\right)^{0.25}\left(R_3^{4.75} - R_2^{4.75}\right) \tag{27}$$

The total friction torque, taking into account turbulence, can be expressed by equation (20), where M_P is now defined by equation (27). The dimensionless form of the total friction torque for turbulent conditions may be expressed as

$$\overline{M}_t = \frac{2M_t \sin\theta\, h_L}{\pi\mu\omega_f R_1^4} = \overline{M}_L + C_2\left(X_3^{4.75} - X_2^{4.75}\right) \tag{28}$$

where

$$C_2 = \frac{2(0.062)}{4.75} f_r \left(\frac{\rho R_1 \omega_f h_P}{\mu} \right)^{0.75} \frac{h_L}{h_P} \tag{29}$$

Differentiating equation (28) with respect to X_2 gives

$$\frac{d\overline{M}_t}{dX_2} = \frac{d\overline{M}_L}{dX_2} + 4.75 C_2 \left(X_3^{3.75} \frac{dX_3}{dX_2} - X_2^{3.75} \right) \tag{30}$$

Therefore, with equations (10), (12), and (24), equations (28) and (30) can be expressed in terms of C_2, X_2, $\overline{F}$, and $\overline{Q}$.

Optimization Procedure

The equations (10), (11), (12), (21), (23), (24), (28), and (30) developed in the analysis were programmed on a digital computer. It is seen from these equations that the friction torque $\overline{M}_t$ and its derivative with respect to X_2 are functions of the dimensionless flow rate $\overline{Q}$, the dimensionless load capacity $\overline{F}$, the dimensionless coefficient C_1 or C_2 (depending on whether the bearing is operating in the laminar or turbulent regime), and the ratio of the outer radius to the inner radius of the inner land X_2.

The problem as defined in the INTRODUCTION is to find the optimal conical hydrostatic bearing configuration for minimum friction torque for laminar and turbulent flow conditions. This means setting $d\overline{M}_t/dX_2$ equal to zero in equations (23) and (30) and finding the values of X_2 which satisfy these equations. The "false position" numerical method was used in finding the optimal value of X_2. When C_1 or C_2, $\overline{F}$, and $\overline{Q}$ are known, the optimal values of X_2 for minimal friction could be obtained for laminar or turbulent flow conditions.

DISCUSSION OF RESULTS

The results are shown in figures 3 to 12. In all these figures the abscissa is the dimensionless flow rate $\overline{Q}$, and for each figure seven curves are shown representing seven values (0.5, 1, 2, 3, 5, 7, and 10) of dimensionless load capacity $\overline{F}$. On the ordinate of these figures, the optimal bearing configuration or the resulting minimum

friction torque is given. For low-speed operation, or when laminar flow exists, the results are shown in figures 3 to 8, where $C_1 = 0,\ 0.4,$ or 0.8. For high-speed operation, when turbulent flow exists, the results are shown in figures 9 to 12, where $C_2 = 0.4$ or 0.8. The values of $\overline{F}$ and $\overline{Q}$ were chosen such that they satisfy inequality (13). The following comments can be made about figures 3 to 12.

(1) A designer is able to find optimal bearing configurations (X_2, X_3, and X_4) for minimum friction torque given the flow rate, load, and angular velocity.

(2) In figures 4 and 11, it is seen that X_3 approaches an asymptote rather quickly. Furthermore, the asymptotic values of X_4 in figure 5 are exactly the asymptotic values of X_3 in figure 4 for a given dimensionless load capacity.

(3) For all the laminar flow cases ($C_1 = 0,\ 0.4,$ and 0.8), it was found that the values of X_3 and X_4 did not change significantly when C_1 changed. Therefore, figures 4 and 5, which are plotted for a $C_1 = 0$, are to be used in obtaining the values of X_3 and X_4, respectively, as long as the pocket flow is laminar ($Re < 1000$).

(4) For all the turbulent flow cases ($C_2 = 0.4$ and 0.8), it was found that X_4 did not change with change of C_2. Therefore, figure 5 may be used in obtaining the value of X_4.

(5) It was found that the addition of the laminar or turbulent pocket friction term in the friction torque expression did not appreciably change the bearing dimensions (values of X_2, X_3, and X_4) for minimum torque. It seems that, no matter how much C_1 and C_2 are increased (within reasonable limits), torque is still less for pocket areas than for the land areas.

(6) Friction torque values rise substantially when the laminar and turbulent pocket friction terms are included, as can be seen from comparing figure 6 with figure 8 and with figures 9 and 12. The torque increase is greatest at high flow rates.

SUMMARY OF RESULTS

Equations for the flow rate, load capacity, and friction torque for a conical hydrostatic bearing were developed. A digital computer program was developed which determined the optimal bearing configuration for minimum friction torque. Design curves showing optimal bearing configurations (radius ratios X_2, X_3, and X_4) or minimum friction torque as a function of dimensionless flow rate were plotted for seven values of dimensionless load capacity. Design curves were shown for both laminar and turbulent flow conditions. The following results were obtained:

1. Friction torque was strongly affected by hydrostatic pocket friction; however, bearing dimensions for a minimum friction design were affected very little by pocket friction.

2. For all laminar-flow cases, the values of X_3 and X_4 did not change significantly with increasing values of friction factor.

3. For all turbulent flow cases, X_4 did not change with increasing values of friction factor; therefore, the value of the friction factor, $C_1 = 0$, determined for laminar flow may be used to obtain the value of X_4 for all turbulent flows.

APPENDIX

SYMBOLS

C_1 dimensionless laminar friction coefficient, $4h_L f_r/h_P$

C_2 dimensionless turbulent friction coefficient, $0.0261\, f_r(\rho R_1 \omega_f h_P/\mu)^{0.75}\, h_L/h_P$

F thrust load

$\overline{F}$ dimensionless thrust load, $F/(\pi p R_1^2)$

f friction factor, $2\tau/\rho V^2$

f_r fraction of area between R_2 and R_3 occupied by hydrostatic pockets

h fluid-film thickness

M fluid-film bearing torque

$\overline{M}$ dimensionless fluid-film bearing torque, $2Mh_1h_2 \sin\theta/(\pi\mu\omega_f)$

M_t total fluid-film bearing torque

p pressure

Q fluid flow

$\overline{Q}$ dimensionless fluid flow, $6\mu Q/(\pi h^3 p \sin\theta)$

R_1 inner radius of inner land

R_2 outer radius of inner land

R_3 inner radius of outer land

R_4 outer radius of outer land

Re Reynolds number, $\rho Vh/\mu$

V relative speed between fluid film bearing surfaces, $r\omega_f$

X_2 R_2/R_1

X_3 R_3/R_1

X_4 R_4/R_1

θ half-angle of conical hydrostatic bearing

μ fluid dynamic viscosity

ρ fluid density

τ fluid-film shear stress

ω_f rotational speed of fluid-film bearing

Subscripts:

L land

P pocket

REFERENCES

1. Rippel, H. C.: Cast Bronze Hydrostatic Bearing Design Manual. Cast Bronze Bearing Institute, Inc., 21010 Center Ridge Road, Cleveland, Ohio 44116.

2. Aston, R. L.; O'Donoghue, J. P. and Rowe, W. B.: Design of Conical Hydrostatic Journal Bearings. Machinery and Production Engineering, vol. 116, no. 2988, Feb. 18, 1970, pp. 250-254.

3. Elwell, R. C. and Sternlight, B.: Theoretical and Experimental Analysis of Hydrostatic Thrust Bearings. Jour. Basic Engr. (Trans. ASME), ser. D, vol. 82, no. 3, 1960, pp. 505-512.

4. Wilcock, D. F. and Winn, L. W.: The Hybrid Boost Bearing—A Method of Obtaining Long Life in Rolling Contact Bearing Applications. Journal of Lubrication Technology (Trans. ASME), ser. F, vol. 92, no. 3, 1970, pp. 406-414.

5. Parker, R. J.; Fleming, D. P.; Anderson, W. J. and Coe, H. H.: Experimental Evaluation of the Series Hybrid Rolling-Element Bearing. NASA TN D-7011.

6. Shinkle, J. N. and Hornung, K. G.: Frictional Characteristics of Liquid Hydrostatic Journal Bearings. Journ. Basic Engr. (Trans. ASME), ser. D, vol. 87, no. 1, 1965, pp. 163-169.

7. Elrod, H. G., Jr. and Ng, C. W.: A Theory for Turbulent Fluid Films and Its Application to Bearings. Jour. Lubr. Tech., vol. 89, no. 3, 1967, pp. 346-362.

8. Constantineseu, V. N. and Galetuse, S.: On the Determination of Friction Forces in Turbulent Lubrication. ASLE Trans., vol. 8, no. 4, 1965, pp. 367-380.

9. Hirs, G. G.: Fundamentals of a Bulk-Flow Theory for Turbulent Lubricant Films. Doctorate Thesis, Delft Univ. of Tech., Delft, Netherlands, 1970.

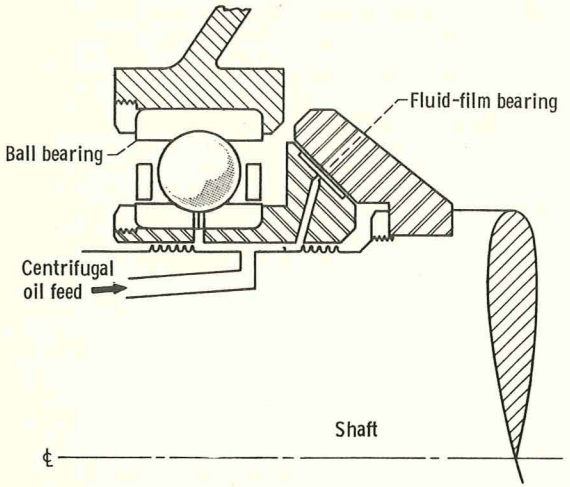

Figure 1. - Schematic diagram of series hybrid fluid-film - rolling-element bearing.

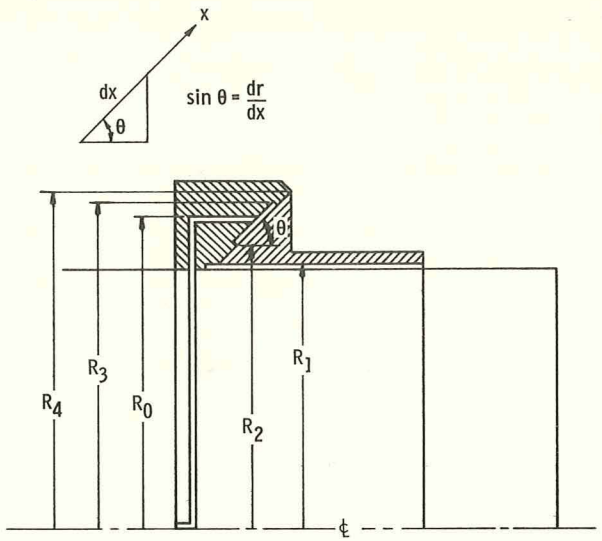

(a) Section view.

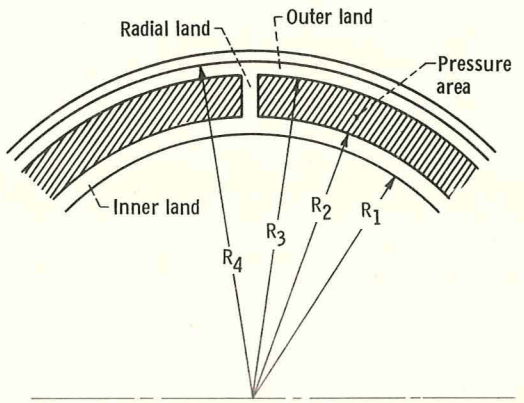

(b) Front view.

Figure 2. - Schematic diagrams of conical hydrostatic bearing design.

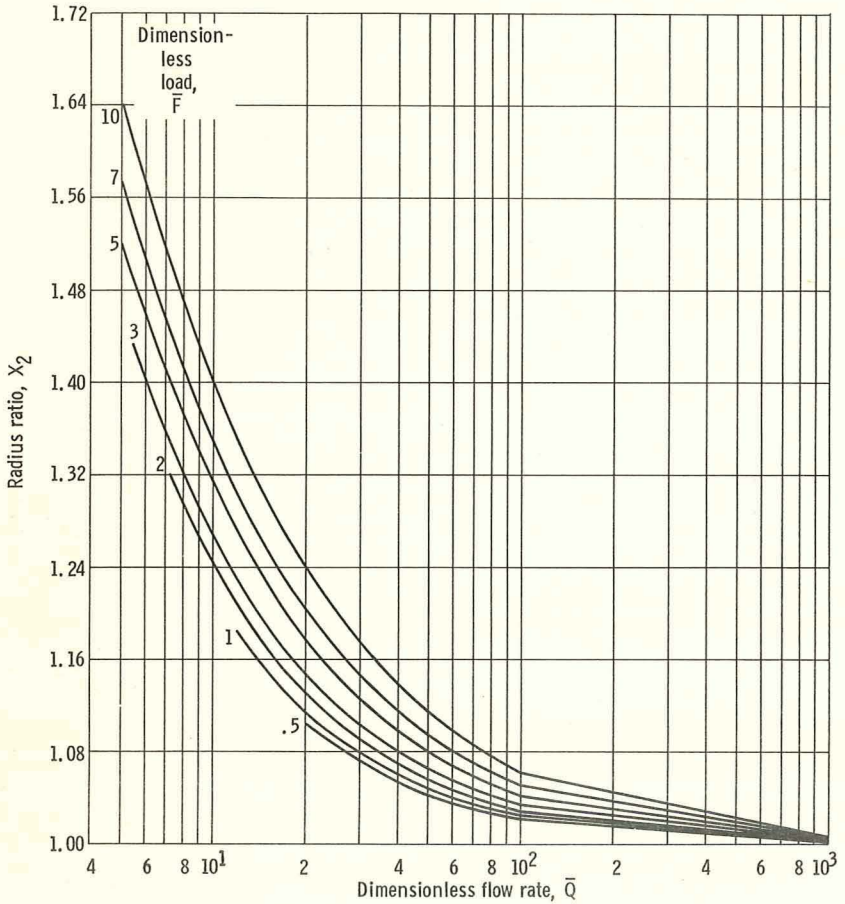

Figure 3. - Effect of flow rate on radius ratio X_2 for optimal bearing. Dimensionless laminar friction coefficient, 0.

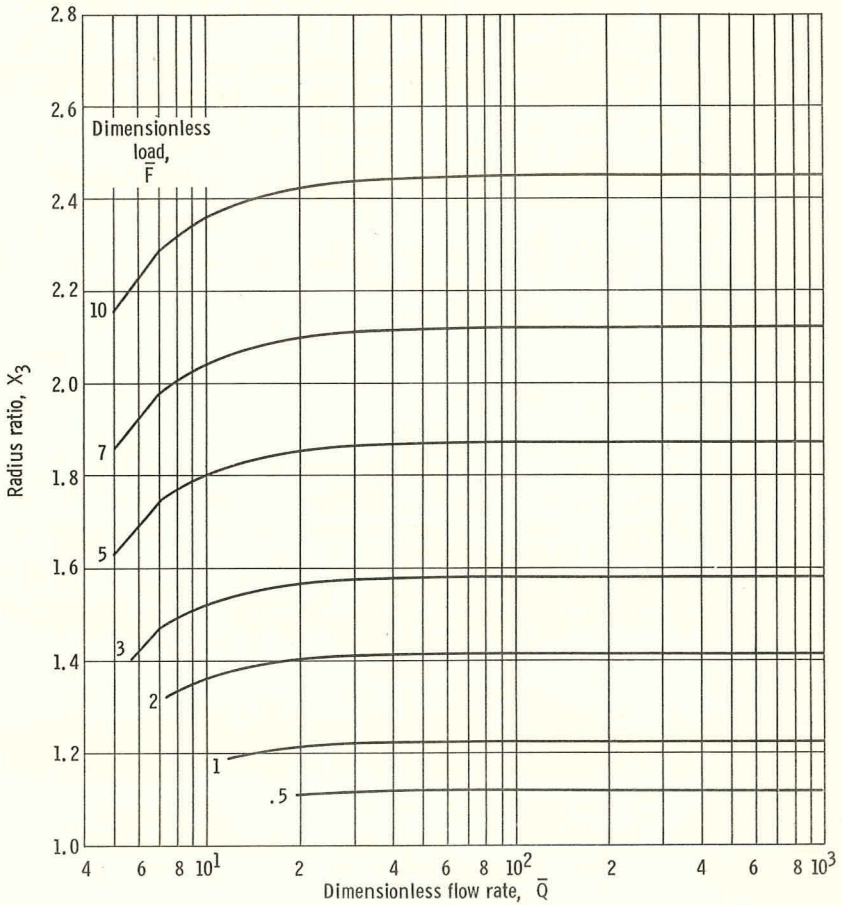

Figure 4. - Effect of flow rate on radius ratio X_3 for optimal bearing. Dimensionless laminar friction coefficient, 0.

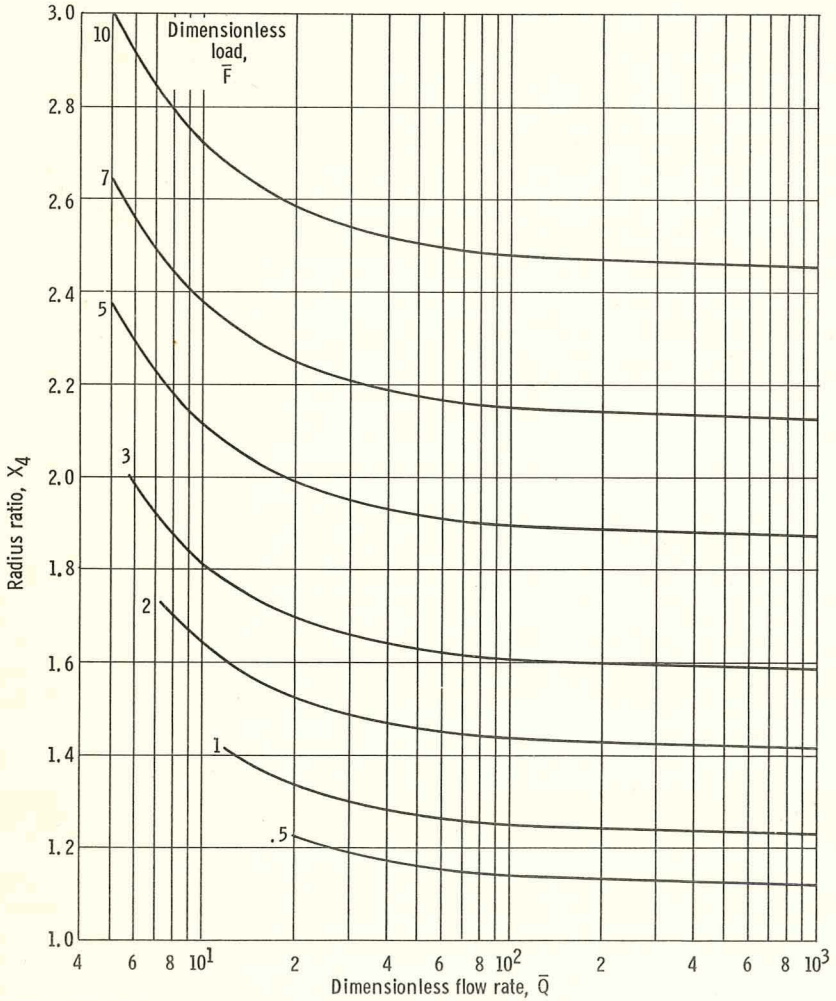

Figure 5. - Effect of flow rate on radius ratio X_4 for optimal bearing. Dimensionless laminar friction coefficient, 0.

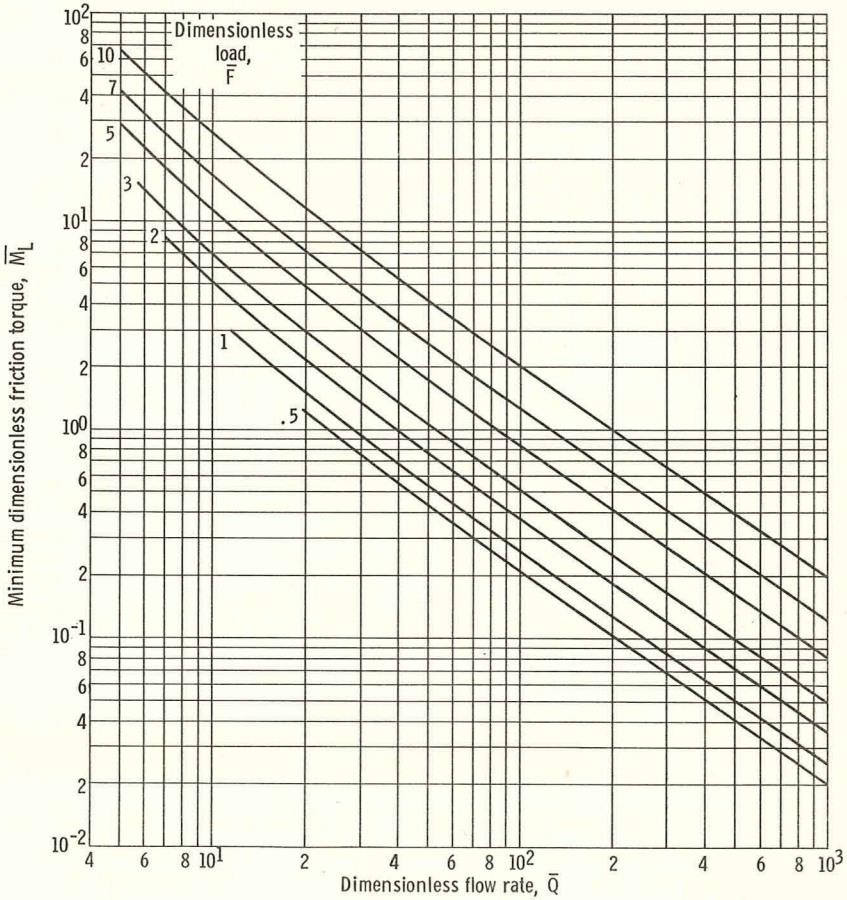

Figure 6. - Effect of flow rate on friction torque for optimal bearing. Dimensionless laminar friction coefficient, 0.

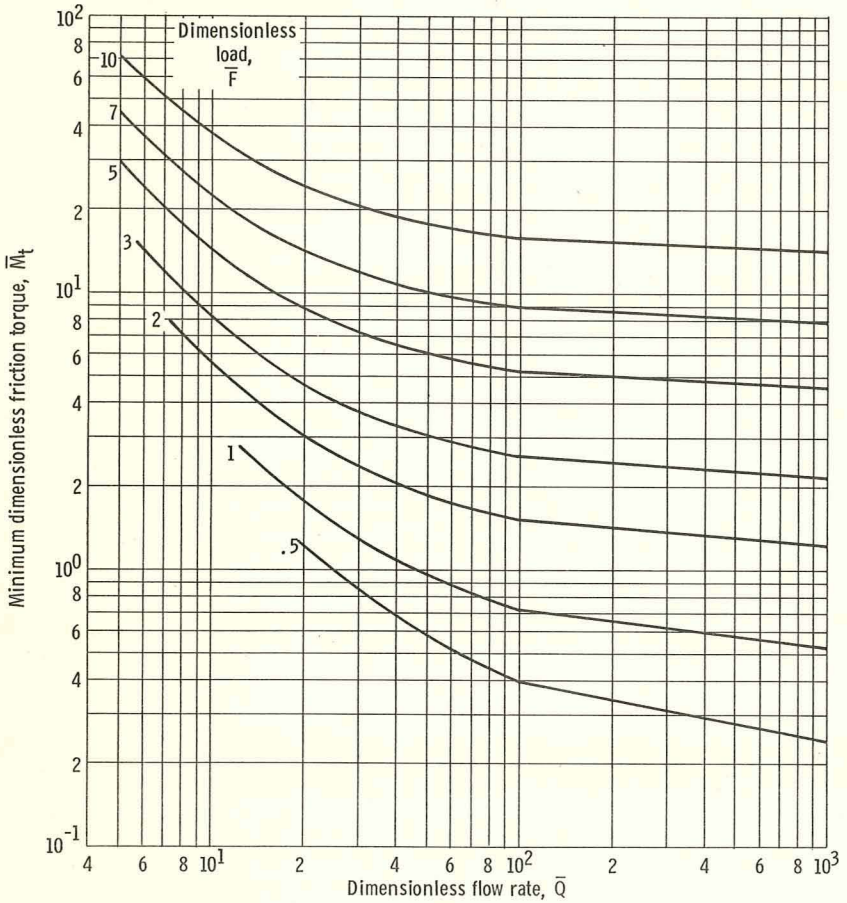

Figure 7. - Effect of flow rate on friction torque for optimal bearing. Dimensionless laminar friction coefficient, 0.4.

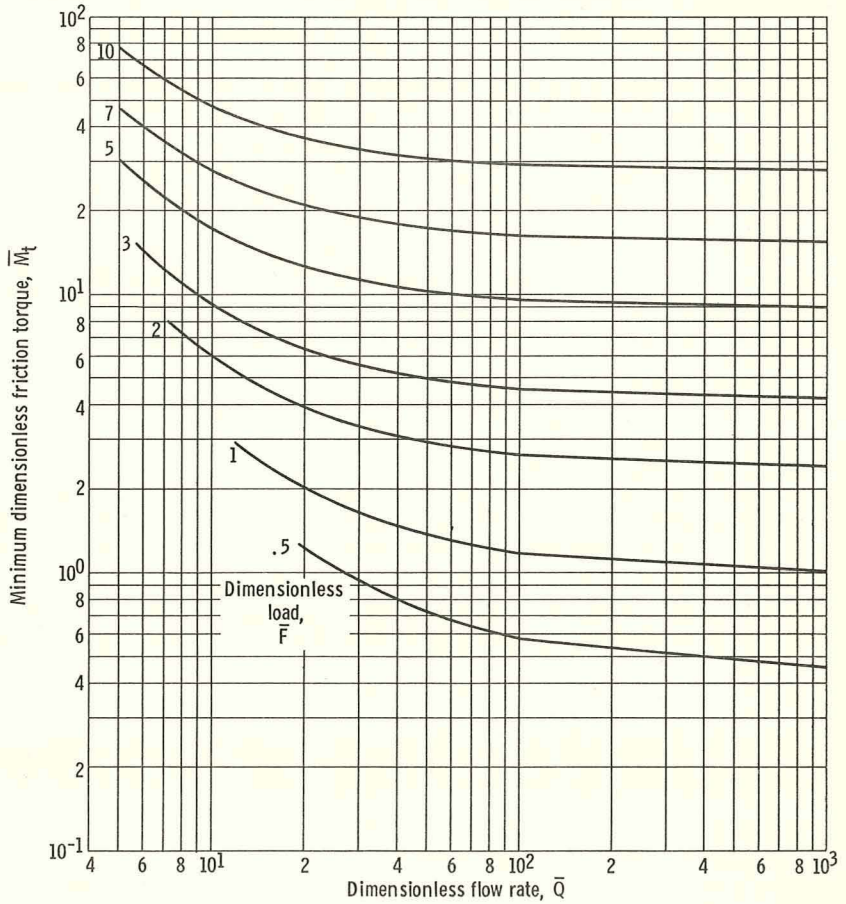

Figure 8. - Effect of flow rate on friction torque for optimal bearing. Dimensionless laminar friction coefficient, 0.8.

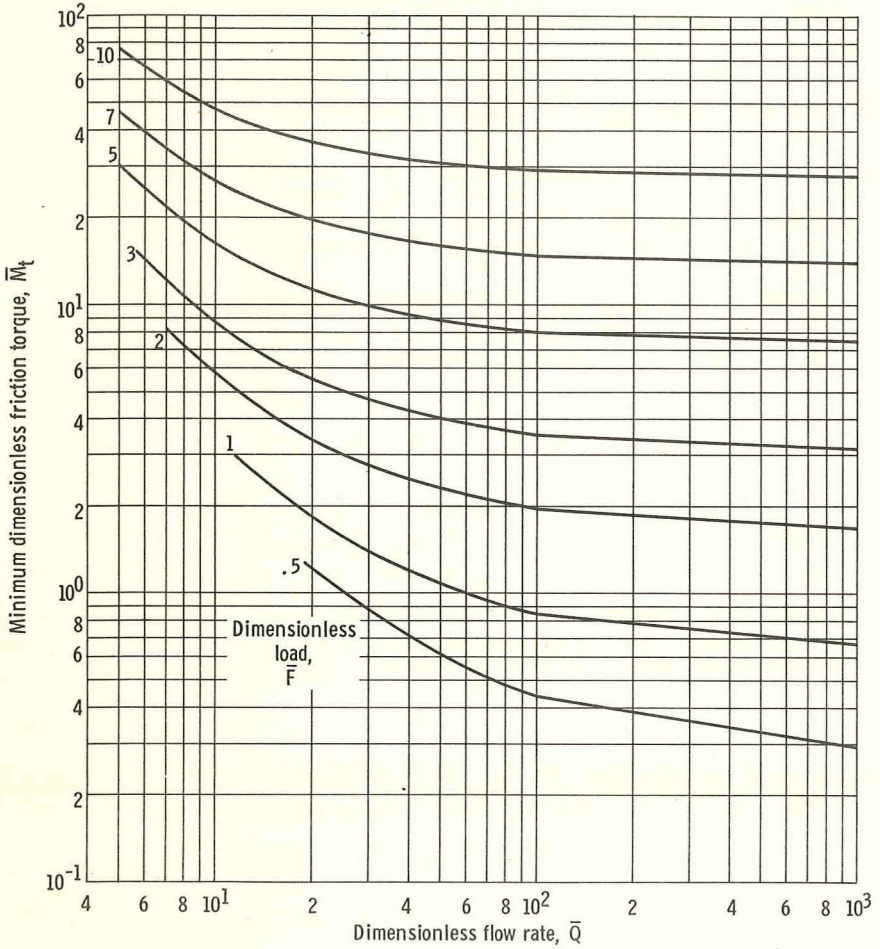

Figure 9. - Effect of flow rate on friction torque for optimal bearing. Dimensionless turbulent friction coefficient, 0.4.

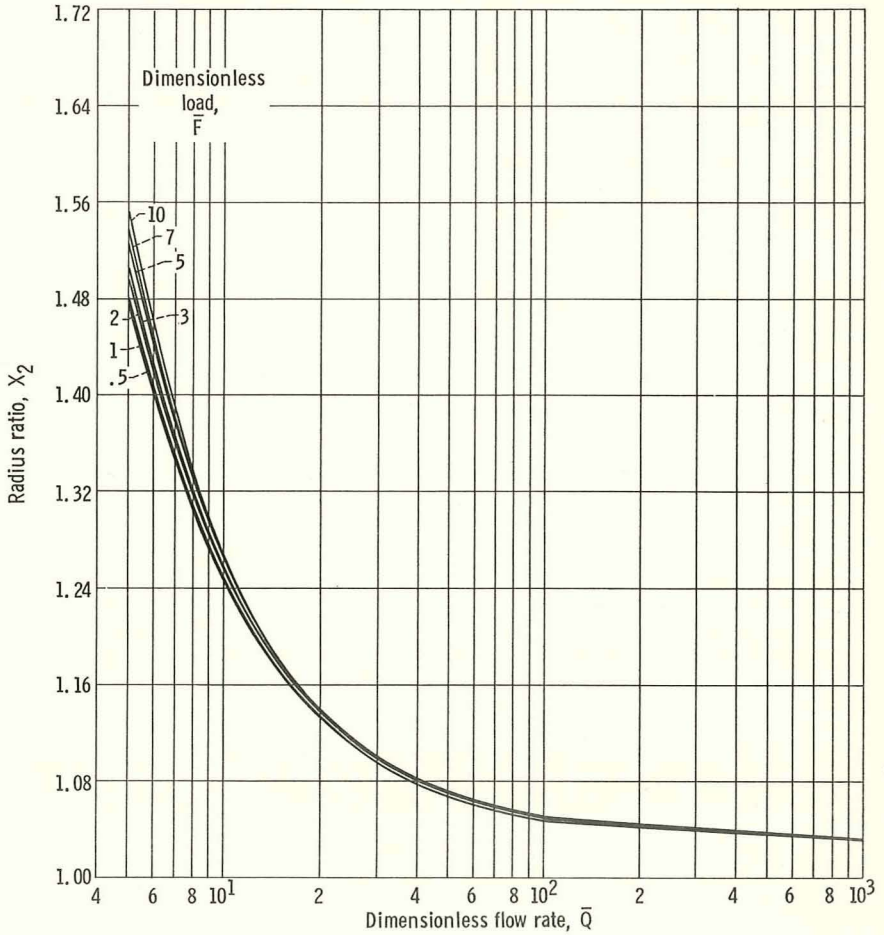

Figure 10. - Effect of flow rate on radius ratio X_2 for optimal bearing. Dimensionless turbulent friction coefficient, 0.8.

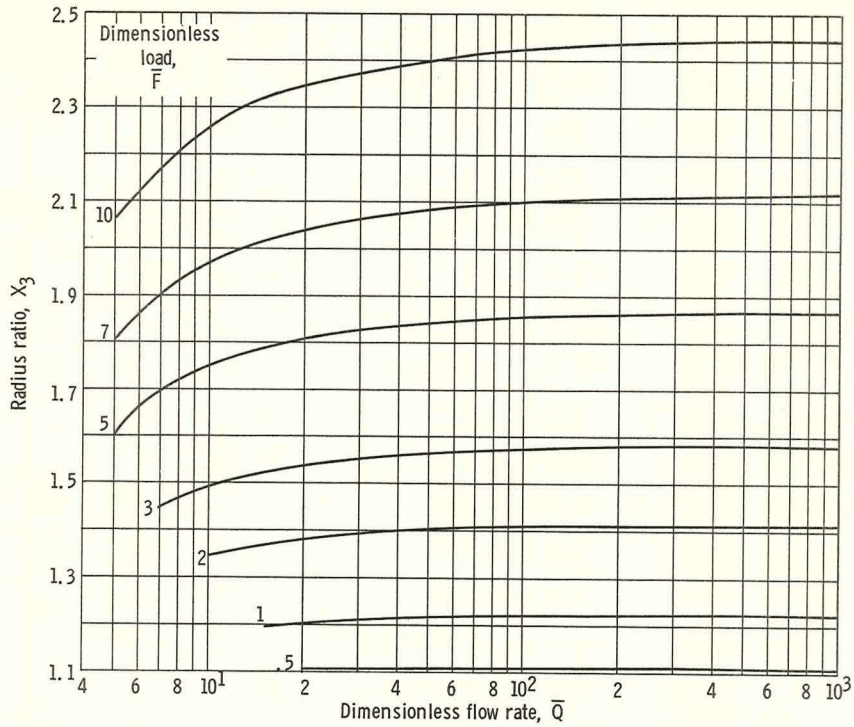

Figure 11. - Effect of flow rate on radius ratio X_3 for optimal bearing. Dimensionless turbulent friction coefficient, 0.8.

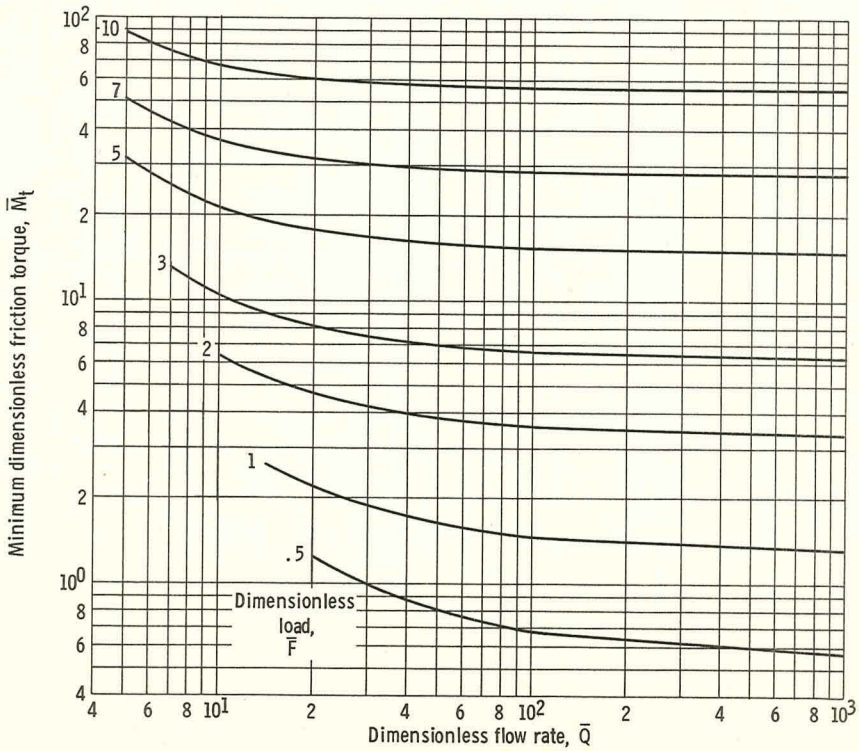

Figure 12. - Effect of flow rate on friction torque for optimal bearing. Dimensionless turbulent friction coefficient, 0.8.